

Asp-99 Donates a Hydrogen Bond Not to Tyr-14 but to the Steroid Directly in the Catalytic Mechanism of Δ^5 -3-Ketosteroid Isomerase from *Pseudomonas putida* Biotype B[†]

Gildon Choi, Nam-Chul Ha, Suhng Wook Kim,[‡] Do-Hyung Kim, Songhee Park, Byung-Ha Oh, and Kwan Yong Choi*

Department of Life Sciences, Center for Biofunctional Molecules and School of Environmental Engineering, Pohang University of Science and Technology, Pohang, Kyungbuk, 790-784, Korea

Received July 8, 1999; Revised Manuscript Received September 23, 1999

ABSTRACT: Δ^5 -3-ketosteroid isomerase (KSI) catalyzes the allylic isomerization of Δ^5 -3-ketosteroids at a rate approaching the diffusion limit by an intramolecular transfer of a proton. Despite the extensive studies on the catalytic mechanism, it still remains controversial whether the catalytic residue Asp-99 donates a hydrogen bond to the steroid or to Tyr-14. To clarify the role of Asp-99 in the catalysis, two single mutants of D99E and D99L and three double mutants of Y14F/D99E, Y14F/D99N, and Y14F/D99L have been prepared by site-directed mutagenesis. The D99E mutant whose side chain at position 99 is longer by an additional methylene group exhibits nearly the same k_{cat} as the wild-type while the D99L mutant exhibits ca. 125-fold lower k_{cat} than that of the wild-type. The mutations made at positions 14 and 99 exert synergistic or partially additive effect on k_{cat} in the double mutants, which is inconsistent with the mechanism based on the hydrogen-bonded catalytic diad, Asp-99 COOH...Tyr-14 OH...C3–O of the steroid. The crystal structure of D99E/D38N complexed with equilenin, an intermediate analogue, at 1.9 Å resolution reveals that the distance between Tyr-14 O η and Glu-99 O ϵ is ca. 4.2 Å, which is beyond the range for a hydrogen bond, and that the distance between Glu-99 O ϵ and C3–O of the steroid is maintained to be ca. 2.4 Å, short enough for a hydrogen bond to be formed. Taken together, these results strongly support the idea that Asp-99 contributes to the catalysis by donating a hydrogen bond directly to the intermediate.

Δ^5 -3-ketosteroid isomerase (KSI)¹ catalyzes the allylic isomerization of the 5,6 double bond of Δ^5 -3-ketosteroids to the 4,5 position at a rate approaching the diffusion limit by an intramolecular transfer of a proton via a dienolate intermediate (*I*; see Figure 1). The KSIs from two different bacterial strains, *Commamonas testosteroni* (previously known as *Pseudomonas testosteroni*) and *Pseudomonas putida* Biotype B, have been extensively studied to understand their catalytic mechanism. Although the two bacterial KSIs share only 34% sequence identity, the three major catalytic residues of Tyr-14, Asp-38, and Asp-99 (the residues are numbered according to *C. testosteroni* KSI

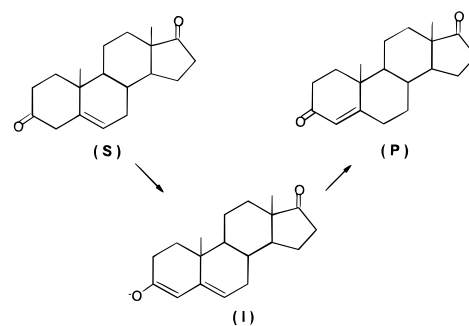


FIGURE 1: Reaction catalyzed by ketosteroid isomerase. The β proton at C-4 is transferred to the β side of C-6 during the isomerization reaction. The substrate (**S**), 5-androstene-3,17-dione, is converted to the product (**P**), 4-androstene-3,17-dione, via the dienolate intermediate (**I**).

throughout the text) are conserved in both of the two isozymes (2, 3). Moreover, the overall three-dimensional structures are remarkably similar to each other (4–6), indicating that the two KSIs may share essentially the same catalytic mechanism.

KSI has been a subject of intensive research for many years as a prototype for studying the enzyme-catalyzed heterolytic cleavage of the C–H bond next to a carbonyl or carboxylic acid group (7). This type of reaction is found ubiquitously in many other enzyme systems. Typical examples include triose phosphate isomerase, citrate synthase

[†] This work was performed by use of the X-ray Facility at Pohang Light Source and was supported by grants from POSTECH research fund, Korea Science and Engineering Foundation, and the academic research fund of Ministry of Education, Korea, and in part by the Research Center for New Biomaterials in Agriculture, Seoul National University.

* To whom correspondence should be addressed. Phone: (82-562) 279-2295. Fax: (82-562) 279-2199. E-mail: kchoi@postech.ac.kr.

[‡] Present address: Division of Hematology, Duke University Medical Center, Durham, NC 27710.

¹ Abbreviations: KSI, Δ^5 -3-ketosteroid isomerase; LBHB, low-barrier hydrogen bond; NMR, nuclear magnetic resonance; 5-AND, 5-androstene-3, 17-dione; equilenin, d-1,3,5(10),6,8-estrapentaen-3-ol-17-one; NOE, nuclear Overhauser effect; IPTG, isopropyl- β -D-thiogalactopyranoside; SDS–PAGE, sodium dodecyl sulfate–polyacrylamide gel electrophoresis; EDTA, ethylenediaminetetraacetic acid; kbp, kilobasepair; ppm, parts per million.

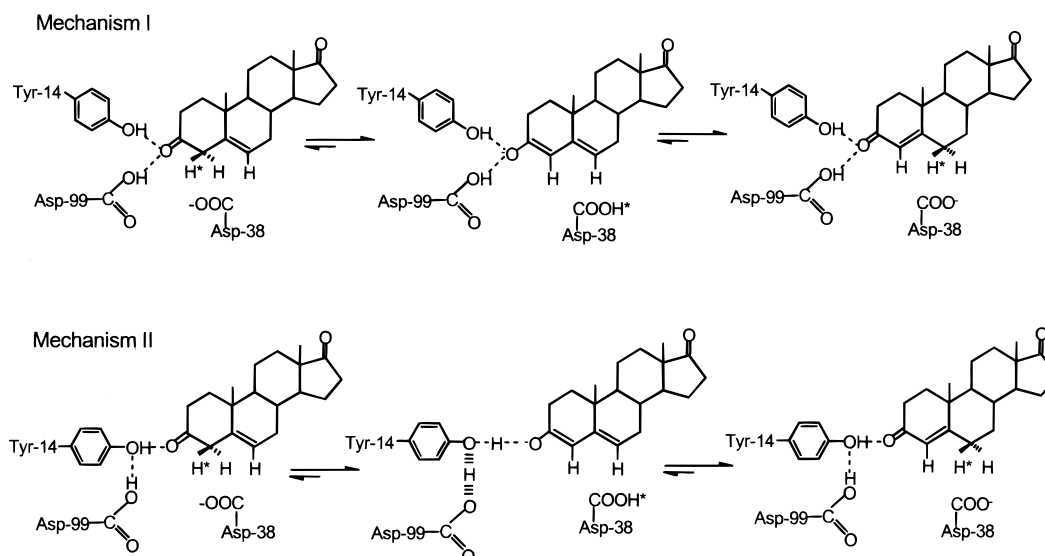


FIGURE 2: Two alternative mechanisms for the stabilization of the reaction intermediate by Tyr-14 and Asp-99 in KSI. Mechanism I: both Tyr-14 OH and Asp-99 COOH form hydrogen bonds with the C3-O of the dienolate intermediate. Mechanism II (catalytic diad mechanism): Asp-99 forms a low-barrier hydrogen bond with Tyr-14 which alone directly donates a hydrogen bond to the intermediate.

and mandelate racemase (7). In the isomerization reaction catalyzed by KSI, Asp-38 acts as the base responsible for shuttling the 4β -proton to the 6β -position in the steroid substrate (8, 9), and a dienolate intermediate generated during catalysis is stabilized by two electrophilic catalysts, Tyr-14 and Asp-99 (5, 6, 10–12). While it has been generally agreed that both Tyr-14 and Asp-99 contribute to catalysis by stabilizing the intermediate through hydrogen bonding, the exact mechanism and the nature of the stabilization by these residues have been rather controversial until recently (4, 5, 10, 11, 13).

The crystal structure of *P. putida* KSI complexed with equilenin (6), an intermediate analogue, has revealed that both Tyr-14 and Asp-99 interact intimately with the bound steroid providing hydrogen bonds directly to C3–O of the steroid (Figure 2, mechanism I). Modeling the substrate into the solution structure of *C. testosteronei* KSI (5) also favors the idea that Asp-99 contributes to catalysis by donating a hydrogen bond directly to the steroid, not via Tyr-14. On the contrary, the results from the NMR spectroscopic studies support the hydrogen-bonded catalytic diad mechanism (mechanism II) in which the reaction intermediate is stabilized by the hydrogen bond from Tyr-14 that is in turn hydrogen bonded to Asp-99; the distance between Tyr-14 and Asp-99 has been found to be sufficiently short for a strong hydrogen bond to be formed on the basis of nuclear Overhauser effects (NOEs) (10, 13), and both proton NMR peaks assigned to Asp-99 COOH and Tyr-14 OH were absent in the Y14F mutant while the D99A mutation induced only the disappearance of its own proton resonance (10). The hydrogen bond between Tyr-14 and Asp-99 in mechanism II has been regarded as a low-barrier hydrogen bond (LBHB) on the basis of its highly deshielded proton NMR peak at 18.15 ppm and its low fractionation factor for deuterium exchange reaction (10, 14). Recently, Cleland et al. (15) adopted mechanism II for exploiting the role of LBHB in the catalytic mechanism of KSI.

To clarify which of the two mechanisms is valid and to identify the actual intermediate stabilization strategy employed by KSI, we have prepared two single mutants, D99L

and D99E, and three double mutants, Y14F/D99E, Y14F/D99N, and Y14F/D99L of *P. putida* KSI and determined their kinetic parameters. The crystal structure of D99E/D38N complexed with equilenin at 1.9 Å resolution has revealed that Glu-99 donates a hydrogen bond to C3–O of the bound steroid but does not form a hydrogen bond with Tyr-14. Our kinetic and structural results clearly demonstrate that Asp-99 donates a hydrogen bond directly to the intermediate analogue and possibly to the dienolate intermediate in the catalytic process of KSI.

MATERIALS AND METHODS

Materials. 5-Androstene-3,17-dione (5-AND), 19-nortestosterone, and equilenin were purchased from Steraloids. The chemicals for the buffer solutions were from Sigma. All the enzymes for DNA manipulation were from Boehringer Mannheim. Oligonucleotides were obtained from Bioneer Inc., Korea. pBluescript SK(–) plasmid was from Stratagen. pKK 223-3 plasmid was from Pharmacia.

Oligonucleotide-Directed Mutagenesis of the KSI Gene. According to the procedure described previously (3), Asp-99 was replaced by a leucine and a glutamate to make D99L and D99E, respectively. The entire coding region of KSI was subcloned into the *EcoRI* and *HindIII* sites of pBluescript SK(–) plasmid (pSK) to construct pSK-D99L and pSK-D99E, respectively. The mutagenesis was performed by use of uracil-containing single-stranded DNA of pSK-KSI as a template and the synthetic oligonucleotide (D99L, 5'-CTG GAT GTC ATC CTT GTG ATG CGC-3'; D99E, 5'-CTG GAT GTC ATC GAA GTG ATG CGC-3'; the underlined nucleotide is the mismatched one) as a primer. For the preparation of the D99E/D38N double mutant, the *EcoRI*/*HindIII* DNA fragments containing the coding region of D38N were also subcloned into the same sites of pSK to construct pSK-D38N, which was subsequently used to prepare the single-stranded pSK-D38N for the additional D99E mutagenesis. Either enzyme digestion or DNA sequencing was carried out to screen the recombinant plasmid containing the desired mutation. The entire nucleotide

sequences of mutant genes were determined to confirm that no other mutations except the desired one occurred during the mutagenesis. The *EcoRI*/*HindIII* DNA fragments containing D99L, D99E, and D99E/D38N mutations were subcloned into the same sites of the pKK 223-3 plasmid to construct the expression vectors of pKK-D99L, pKK-D99E, and pKK-D99E/D38N, respectively. For the preparation of double mutants of Y14F/D99E, Y14F/D99N, and Y14F/D99L, the DNA fragments containing the mutations of D99E, D99N, and D99L were digested with *EcoRV* and *HindIII* and ligated into the sites of *EcoRV* and *HindIII* of pSW-Y14F (3) containing the Y14F mutation, respectively.

Overexpression and Purification of Mutant Isomerases. The procedures for overexpression and purification of KSI were carried out as described previously with a slight modification (3, 16). The cultures were grown in 500 mL of Luria-Bertani medium containing 250 mg of ampicillin/L at 37 °C until the OD₆₀₀ reached 0.6. After the addition of IPTG up to the final concentration of 0.75 mM, the bacterial cells were cultured at 37 °C for an additional 8 h, harvested by centrifugation, and then resuspended in 25 mL of 40 mM phosphate buffer, pH 7.0, containing 1 mM EDTA and 20 mM β -mercaptoethanol. The purification of the wild-type and the mutant enzymes was carried out with a deoxycholate affinity chromatography as a principle step according to the procedures described previously (3, 16). The purified enzymes showed homogeneous single bands on SDS-PAGE. Both the wild-type and the mutant enzymes exhibited similar mobilities on SDS-PAGE corresponding to a molecular mass of 14 kDa of the KSI monomer (data not shown). The concentrations of purified enzymes were determined by the colorimetric assay of Bradford (17) and confirmed by the measurement of the band intensity on SDS-PAGE gel by use of an imaging densitometer (Bio-Rad GS-700) and a program, Molecular Analyst/PC (Bio-Rad Windows software).

Determination of Kinetic Constants K_m , K_i , and k_{cat} . Reactions were carried out in a solution of 3 mL containing 34 mM potassium phosphate, pH 7.0, 2.5 mM EDTA, 5-AND, and enzymes as described previously (3). The final concentration of methanol in the reaction mixture was 3.3 vol %. The reactions were initiated by the addition of enzyme, and the amount of the reaction product was determined spectrophotometrically by measuring the absorbance at 248 nm. All reaction rates were corrected for the spontaneous isomerization, which was measured prior to the addition of enzymes. Enzymes were diluted appropriately in a solution containing 40 mM potassium phosphate, 2.5 mM EDTA, pH 8.0, and 1% bovine serum albumin just prior to use. All assays were performed at 25 °C. Kinetic parameters such as k_{cat} , K_m , and K_i were obtained by analyzing the data using Lineweaver-Burk reciprocal plots under the assay conditions in which the substrate concentrations were 11.6, 34.9, 58.2, 81.5, and 116.4 μ M, respectively. Mean values (\pm standard deviations) from three independent determinations were obtained for the comparison of kinetic parameters. For inhibition experiments, the activity of KSI was measured under the same conditions as above except that the methanol concentration was raised to 3.7% by the addition of inhibitors in methanol to the reaction mixture.

Crystallization. Crystallization of D99E/D38N complexed with equilenin, an intermediate analogue, was accomplished

Table 1: X-ray Crystallographic Determination of the D99E/D38N Mutant KSI Complexed with Equilenin, an Intermediate Analogue

resolution (\AA)	1.9
R_{sym} (%)	4.6
data completeness, $F > 1\sigma$ (%)	86.6
R_{standard} (%)	20.4
R_{free} (%)	25.9
total number of atoms	982
water molecules	69
average B -factor (\AA^2)	25.7
rmsd bond length (\AA)	0.016
rmsd bond length (deg)	1.790
Ramachandran plot (%)	
most favored region	88.3
additional allowed region	10.7
disallowed regions	0.5

by the procedures as described previously with a slight modification (6). The D99E/D38N mutant was crystallized instead of the D99E mutant to enhance the binding affinity of the steroid to KSI. The KSI solution was prepared at 20 mg/mL concentration in 50 mM Tris-Cl, pH 7.0, containing 20 mM β -mercaptoethanol, and 70 μ L of this solution was mixed with 2 μ L of equilenin in dimethyl sulfoxide. The crystals of the complex were grown from 1.1 M ammonium acetate and 0.1 M sodium acetate, pH 4.6, by the hanging drop vapor diffusion method at 22 °C. The resulting crystals were found to have C2 space group symmetry with unit cell dimensions of $a = 89.04 \text{ \AA}$, $b = 72.42 \text{ \AA}$, $c = 51.24 \text{ \AA}$, and $\beta = 90.9^\circ$. The detailed information on the crystals of the D99E/D38N mutant complexed with equilenin is presented in Table 1.

Data Collection, Structure Determination, and Refinement. All diffraction data (86.6% completeness up to 1.9 \AA) were measured on a DIP2000 area detector with graphite monochromated CuK α X-rays generated by a MacScience M18XHF rotating anode generator operated at 90 mA and 50 kV at room temperature. Data reduction, merging, and scaling were accomplished with the programs DENZO and SCALEPACK (18). The structure of D99E/D38N complexed with equilenin² was determined by use of the coordinates of the D38N/equilenin complex which had been deposited at the Brookhaven Protein Data bank as a code number 4TST. The refinement was carried out with the program X-PLOR version 3.851.

RESULTS

Kinetic Analysis. The k_{cat} and K_m values of mutant enzymes for 5-AND as a substrate were compared with those of the wild-type enzyme (Table 2). All the mutations made at positions 14 and 99 do not affect significantly the K_m values of the mutants compared with that of the wild-type. The k_{cat} value of D99L was ca. 125-fold lower than that of the wild-type enzyme, consistent with the proposal that Asp-99 plays a crucial role in catalysis. The similar k_{cat} values between D99A (2) and D99L imply that the extra space generated by the D99A mutation near the catalytic center does not influence significantly the catalytic power of the enzyme. In contrast to D99A and D99L, D99E exhibited the nearly comparable k_{cat} and k_{cat}/K_m values to those of the wild-type,

² The atomic coordinates of the D99E/D38N mutant complexed with equilenin have been deposited with the entry code 1CQS at the Brookhaven Protein Data Bank.

Table 2: Kinetic Parameters of the Wild-Type and Its Mutant KSIs^a

enzyme	k_{cat} (s ⁻¹)	K_{m} (μM)	$k_{\text{cat}}/K_{\text{m}}$ (M ⁻¹ s ⁻¹)	relative k_{cat}	relative $k_{\text{cat}}/K_{\text{m}}$
wild-type	27 900 \pm 300	50.3 \pm 1.7	5.5×10^8	1.0	1.0
Y14F	11.5 \pm 1.5	26.9 \pm 3.9	4.3×10^5	10 ^{-3.4}	10 ^{-3.1}
D99E	19 000 \pm 600	61.6 \pm 4.6	3.1×10^8	0.68	0.56
D99N	5709 \pm 271 ^b	36.8 \pm 0.7 ^b	1.6×10^8	0.27	0.29
D99A	254 \pm 15 ^b	31.8 \pm 2.0 ^b	8.0×10^6	10 ^{-2.0}	10 ^{-1.8}
D99L	220 \pm 8.9	25.8 \pm 0.8	8.7×10^6	10 ^{-2.1}	10 ^{-1.8}
Y14F/D99E	3.0 \pm 0.1	48.1 \pm 3.3	6.2×10^4	10 ^{-4.0}	10 ^{-3.9}
Y14F/D99N	0.71 \pm 0.05	47.5 \pm 1.0	1.5×10^4	10 ^{-4.6}	10 ^{-4.6}
Y14F/D99L	0.67 \pm 0.01	98.2 \pm 6.9	6.8×10^3	10 ^{-4.6}	10 ^{-4.9}

^a The assays were performed in 34 mM potassium phosphate buffer containing 2.5 mM EDTA, pH 7.0 (final concentration of methanol was 3.3%). ^b Data from Kim et al. (2).

indicating that Glu-99 in this mutant stabilizes the dienolate intermediate as efficiently as Asp-99 in the wild-type.

To clarify the interactions between Tyr-14 and Asp-99 in the active site, we prepared the double mutants of Y14F/D99E, Y14F/D99N, and Y14F/D99L and compared their kinetic parameters with those of the respective single mutants. All the double mutants exhibited decreased k_{cat} values relative to Y14F. Especially, the k_{cat} values of Y14F/D99N and Y14F/D99L were 17-fold lower compared with that of Y14F. It is noticeable that the k_{cat} value of Y14F/D99N was similar to that of Y14F/D99L even though D99N exhibits a 26-fold higher k_{cat} value than that of D99L (Table 2). This result implies that the Y14F mutation can affect the hydrogen bonding of Asn-99 to the intermediate in Y14F/D99N. The k_{cat} value of Y14F/D99L (0.67 ± 0.01 s⁻¹) was lower than that of Y14F (11.5 ± 1.5 s⁻¹) but higher than the expected k_{cat} value (0.19 s⁻¹) from the complete independent actions of the Y14F and the D99L mutations on k_{cat} in Y14F/D99L. The partial additive effects of the two mutations imply that Asp-99 is not totally dependent on Tyr-14 for catalysis. The k_{cat} value of Y14F/D99N (0.71 ± 0.01 s⁻¹) was found to be lower than the expected (3.0 s⁻¹) from the independent actions of the Y14F and the D99N mutations, indicating that the D99N mutation interacts synergistically with the Y14F mutation in catalysis by Y14F/D99N.

Three-Dimensional Structure of the D99E/D38N Mutant KSI Complexed with Equilenin. To clarify the geometry of the hydrogen bond from Asp-99 on the structural basis, the crystal structure of D99E/D38N complexed with equilenin has been determined at 1.9 Å resolution. Electron densities for all the residues including Tyr-14, Asp-38, and Glu-99 as well as the bound steroid were clearly defined except some residues in flexible loops. The overall structure was very similar to that of D38N complexed with the steroid (Figure 3). The root-mean-square (rms) difference for all the α -carbon atoms between the structures of D38N and D99E/D38N was obtained to be 0.24 Å, indicating that there are no significant structural differences between these two enzymes.

When the two structures are superimposed with each other, the steroid bound to D99E/D38N was found to be slightly displaced relative to that bound to D38N. However, this slight displacement of the bound steroid did not lead to the alteration of the hydrogen bond geometry between the steroid and catalytic side chains; the hydroxyl group of Tyr-14 in the structure of D99E/D38N provides virtually the same hydrogen bond to the bound equilenin as in D38N (Figure 4). Although the side chain of a glutamate is longer by an

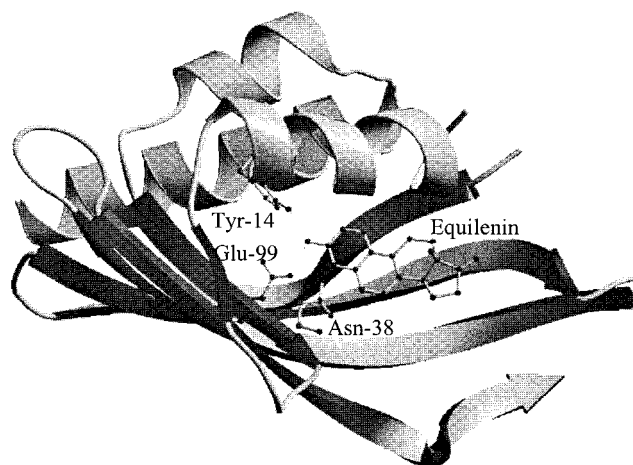


FIGURE 3: Ribbon diagram of the three-dimensional structure of the D99E/D38N mutant KSI complexed with equilenin. Only one of the two monomers in the D99E/D38N mutant is shown in this figure and some structural components are omitted for a clear demonstration of the bound steroid. The side chains of Tyr-14, Asn-38 and Glu-99 as well as the bound steroid in D99E/D38N are shown in ball-and-stick model. The figure was drawn by use of Molscript program (20).

additional methylene group than an aspartate, Glu-99 in D99E/D38N was found to be able to form a hydrogen bond with the bound steroid similarly to Asp-99 in D38N (Figure 4). The hydrogen-bonding distances between Tyr-14 O η and C3–O of equilenin and between Glu-99 O ϵ and C3–O of equilenin were determined to be ca. 2.5 and 2.4 Å, respectively (Table 3). Meanwhile, the distance between Tyr-14 O η and Glu-99 O ϵ was found to be ca. 4.1 Å, excluding any possibility of a direct hydrogen bond between them (Table 3). The mean absolute error in atomic positions of D99E/D38N complexed with the steroid was obtained to be 0.25 Å when estimated by Luzzati plots (19) (Figure 5). Even though we allow this coordinate error in the measured distances, Glu-99 O ϵ cannot provide a hydrogen bond directly to Tyr-14 O η . Little possibility of a hydrogen bond between Glu-99 O ϵ and Tyr-14 O η in D99E/D38N strongly supports that Asp-99, whose side chain is shorter by one methylene group than that of Glu-99, does not provide a hydrogen bond to Tyr-14.

Affinities of the Wild-Type and D99E Mutant KSI for the Steroid Inhibitor. The K_i for equilenin was very similar between the wild-type and D99E, suggesting that the slight displacement of the steroid observed in D99E/D38N may not affect significantly the affinity of D99E for equilenin (Table 4). The preservation of the hydrogen bonds from both

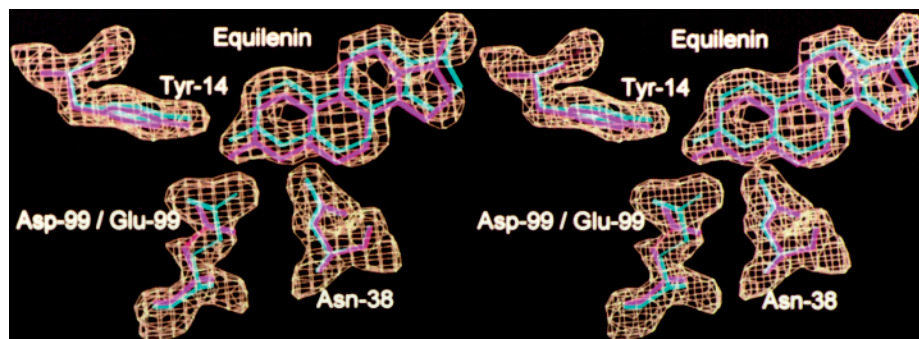


FIGURE 4: Stereodiagram of the superimposed structures of the D38N and the D99E/D38N mutant KSIs complexed with equilenin, respectively. This stereodiagram shows the quality of the $2F_o - F_c$ electron density in the active center of the D38N and D99E/D38N mutant KSIs complexed with equilenin, respectively. The equivalent atoms of all residues were utilized to superimpose the two structures. Three major catalytic residues and the bound steroid are shown for D99E/D38N in cyan color and for D38N in coral color. The O—O distances between the catalytic residues and the steroid are listed in Table 3. The figure was drawn by use of program O (21).

Table 3: Interatomic Distances Among the Oxygen Atoms of the Catalytic Residues and the Bound Steroid^a

	D38N	D99E/D38N
from Tyr-14 O η to C3 O of equilenin	2.66 Å (1)	2.49 Å (1)
	2.56 Å (2)	2.46 Å (2)
from Asp-99 O δ (or Glu-99 O ϵ) to C3 O of equilenin	2.56 Å (1)	2.42 Å (1)
	2.53 Å (2)	2.31 Å (2)
from Tyr-14 O η to Asp-99 O δ (or Glu-99 O ϵ)	4.18 Å (1)	4.19 Å (1)
	4.14 Å (2)	4.27 Å (2)

^a The shortest distance is presented for the hydrogen bond involving the carboxyl group of Asp-99 or Glu-99 in the table. The figure in parenthesis indicates the number of the protomer of KSI. The mean absolute errors in atomic position of D38N and D99E/D38N complexed with equilenin are 0.26 and 0.25 Å, respectively, when estimated by Luzzati plots as shown in Figure 5.

Tyr-14 and Glu-99 to equilenin might be responsible for the high affinity of D99E for the steroid. In contrast, the K_i of D99E for 19-nortestosterone, a product analogue, was significantly increased by ca. 7-fold compared with that of the wild-type enzyme, implying that the steroid may not interact optimally with Tyr-14 and Glu-99.

DISCUSSION

The analysis of the kinetic constants for several mutant enzymes has allowed us to clarify the role of Asp-99 in catalysis. The replacement of Asp-99 with a glutamate results in a similar k_{cat} to that of the wild-type. This similarity in k_{cat} for the wild-type and D99E suggests that the interactions crucial for catalysis should be preserved in D99E. The crystal structure of D99E/D38N has revealed that the three catalytic residues, Tyr-14, Asp-38, and Glu-99, are suitably located with respect to the bound steroid for efficient catalysis. Especially, both Tyr-14 and Glu-99 are shown to provide hydrogen bonds directly to C3—O of the steroid in the structure. According to the catalytic diad mechanism, the hydrogen bond between Glu-99 O ϵ and Tyr-14 O η in D99E would be prominent since the carboxylate group of Glu-99 can approach more closely at least 1.5 Å toward Tyr-14 O η than the carboxylate of Asp-99 in the wild-type enzyme. Contrary to this expectation, the nearest distance between Glu-99 O ϵ and Tyr-14 O η in D99E/D38N is not reduced and maintained nearly constant as in D38N (Table 3). These results strongly suggest that the direct hydrogen bonding between Glu-99 and Tyr-14, and probably between Asp-99 and Tyr-14, is unfavorable in the catalytic mechanism. In

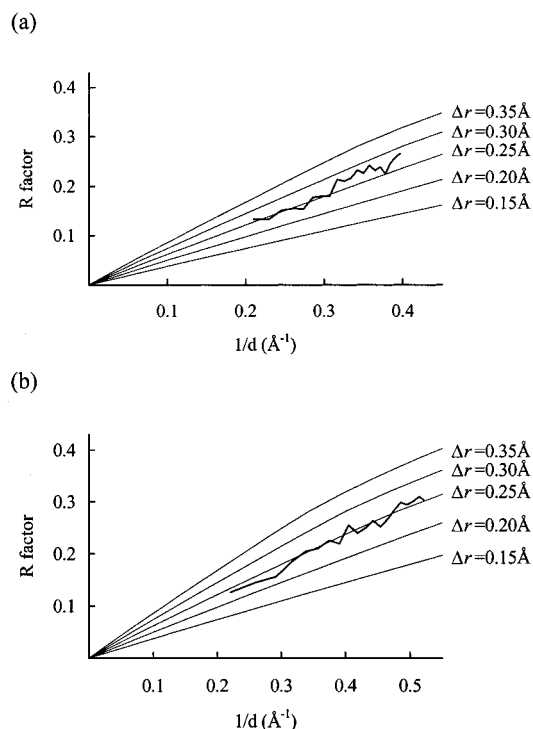


FIGURE 5: Luzzati plots showing the mean absolute errors in atomic positions for the structures of (a) D38N and (b) D99E/D38N complexed with equilenin, respectively. The heavy line indicates the R -factor distribution of the observed structural factors. The thin lines represent the R factor estimated theoretically with mean absolute displacements (Δr) of 0.15, 0.20, 0.25, 0.30, and 0.35 Å, respectively, in atomic position. The calculated mean absolute errors in atomic positions of the D38N and D99E/D38N mutant KSIs are 0.26 and 0.25 Å, respectively.

contrast, it has been proposed that Tyr-14 and Asp-99 are located closely enough for a strong hydrogen bond to be formed on the basis of NOEs (10). However, the distances based on weak NOEs or on the NOEs involving rapidly exchanging OH protons are difficult to be determined with such a high accuracy as to discriminate between mechanism I and mechanism II as pointed out by Pollack and co-workers (11).

The simultaneous mutations made at positions 14 and 99 have made it possible to clarify the interactions between Tyr-14 and Asp-99 in more detail. The double mutants of Y14F/D99E, Y14F/D99N, and Y14F/D99L exhibited the decreases in k_{cat} compared with that of Y14F (Table 2), indicating that

Table 4: Affinities of the Wild-Type and the D99E Mutant KSI for the Steroid Inhibitors^a

steroid	enzyme	K_i^b
equilenin	wild-type	1.8 ± 0.6
	D99E	2.4 ± 0.7
19-nortestosterone	wild-type	4.6 ± 0.2
	D99E	31.3 ± 0.7

^a The assays were performed in 34 mM potassium phosphate buffer containing 2.5 mM EDTA (final concentration of methanol is 3.7%).

^b Values are mean \pm standard deviations from three independent experiments. Both steroids inhibited the activity of KSI in a competitive fashion.

the effect of the respective single mutations on k_{cat} in the double mutant is either synergistic or partially additive. The catalytic diad as suggested in mechanism II is reminiscent of the well-known catalytic triad of serine, histidine, and aspartic acid in the serine proteases in which the formation of a LBHB between His and Asp may facilitate the nucleophilic attack on the acyl carbonyl group in the substrates by the β -OH group of a catalytic serine (22). In subtilisin, one of the serine proteases, an additional mutagenesis in S221A to replace either His-64 or Asp-32 by an alanine causes essentially no further decrease in k_{cat} below that of S221A (23), indicating that the additional mutation of H64A or D32A in S221A exhibits no additive effect on k_{cat} in H64A/S221A and D32A/S221A. If Asp-99 COOH is connected directly to Tyr-14 OH by a hydrogen bond in KSI, the k_{cat} values of the double mutants of Y14F/D99E, Y14F/D99N, and Y14F/D99L would not be decreased further below that of Y14F exhibiting essentially no additive effect on k_{cat} as shown in the mutational analyses for subtilisin. The synergistic or partially additive effect observed in Y14F/D99N and Y14F/D99L of *P. putida* KSI strongly suggests that the arrangement of Asp-99 is not like that of the catalytic diad in mechanism II.

The k_{cat} of Y14F/D99N would be expected to be significantly higher than that of Y14F/D99L, since D99N that retains some hydrogen-bonding capability exhibits a 26-fold higher k_{cat} than D99L. Contrary to the expectation, the Y14F mutation rendered the catalytic activity of Y14F/D99N similar to that of Y14F/D99L, indicating that the Y14F mutation not only abolishes the hydrogen-bonding capability of Tyr-14 but also hinders the contribution of Asp-99 to catalysis. The similar k_{cat} of Y14F/D99N to that of Y14F/D99L can be explained by the effect of the Y14F mutation

on the hydrogen bond network. Tyr-14 and Asp-99 are components of a hydrogen bond network, Asp-99 COOH \cdots O of a water \cdots Tyr-14 OH \cdots Tyr-55 OH, at the active site in the crystal structure of *P. putida* KSI in the native form (6) (Figure 6). The Y14F mutation eliminating the hydroxyl group located at the center of the hydrogen bond network (Figure 6) is expected to perturb the organization of the groups involved in the network including Asp-99 COOH. Since the right positioning of an electrophilic catalyst adjacent to the C3-O of the steroid may be important for the efficient catalysis by KSI (7), the resulting disorganization of Asp-99 by the Y14F mutation would affect the role of Asp-99 in catalysis and its interaction with the steroid. The simultaneous disappearance of both 18.2 and 11.6 ppm proton peaks assigned to Asp-99 COOH and Tyr-14 OH, respectively, upon the Y14F mutation in the NMR study of *C. testosteronei* KSI (10) might also be interpreted as the consequence of the perturbation of Asp-99 COOH by the Y14F mutation in the hydrogen bond network.

The involvement of Asp-99 in the formation of an LBHB between Tyr-14 and Asp-99 has been inferred by the absence of the 18.2 ppm proton peak in the spectrum of the D99A mutant of *C. testosteronei* KSI. However, the corresponding 16.3 ppm proton peak of *P. putida* KSI was found to be still present in the spectrum of the D99L mutant (24), suggesting that the 16.3 ppm proton peak might originate from a hydrogen bond between Tyr-14 OH and C3-O of equilenin. The 2.26 Å crystal structure of *C. testosteronei* KSI complexed with equilenin also excludes a possibility of an LBHB between Tyr-14 and Asp-99 (24).

One of the intriguing features of D99E in its interaction with the steroid is that its affinity for 19-nortestosterone is markedly reduced, while its affinity for equilenin and the catalytic activity are almost the same as those of the wild-type (Table 4). Accordingly, the catalytic mechanism of D99E would be better assessed by the intermediate analogue rather than by the product analogue since the poor interaction of D99E with 19-nortestosterone does not lead to a significant reduction in k_{cat} for the mutant. The binding modes of the two steroids will be different from each other since they are different in the A and B ring structures as well as in the orientation of the C3-O of the steroid, which interacts intimately with the catalytic residues of the enzyme. It might be possible that the intimate interaction between Tyr-14 and Asp-99 observed in the solution structure of *C. testosteronei*

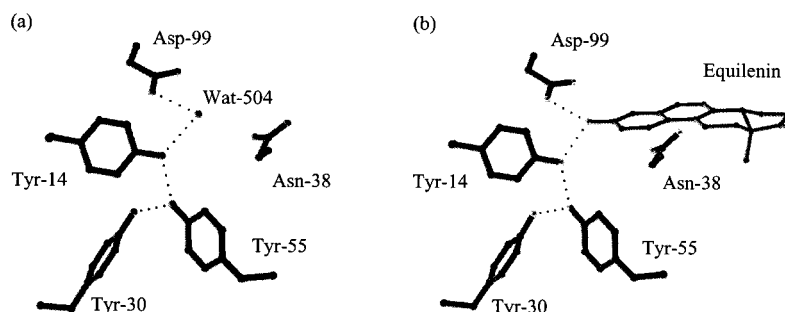


FIGURE 6: Hydrogen bond network at the active site of *P. putida* KSI with (a) and without (b) equilenin. A water molecule is a part of the network in the native structure of *P. putida* KSI. The water oxygen is replaced by C3-O of equilenin when the steroid is bound to the enzyme. Tyr-30 which is a part of the hydrogen bond network in *P. putida* KSI is homologously substituted by a phenylalanine residue in the *C. testosteronei* KSI.

KSI (13) is due to the difference in the binding mode of 19-nortestosterone toward the enzyme from that of equilenin.

In conclusion, we have shown that the high catalytic activity of D99E could be attributed to a hydrogen bond geometry at the active site similar to that of the wild-type. The Glu-99 in D99E provides a similar hydrogen bond to C3=O of the intermediate analogue as provided by Asp-99 in the wild-type. The effects of the mutations made at positions 14 and 99 on k_{cat} in the double mutants could be better explained by the absence of a hydrogen bond between Tyr-14 and Asp-99. These findings strongly support the idea that both Tyr-14 and Asp-99 donate hydrogen bonds directly to the steroid in *P. putida* KSI.

ACKNOWLEDGMENT

We are very grateful to Dr. Byeung Doo Song and Mr. Sung Goo Yun for helpful discussion and comments, and Do Soo Jang for experimental assistance with the preparation of affinity columns.

REFERENCES

1. Schwab, J. M., and Henderson, B. S. (1990) *Chem. Rev.* 90, 1203–1245.
2. Kim, S. W., Joo, S., Choi, G., Cho, H.-S., Oh, B.-H., and Choi, K. Y. (1997) *J. Bacteriol.* 179, 7742–7747.
3. Kim, S. W., and Choi, K. Y. (1995) *J. Bacteriol.* 177, 2602–2605.
4. Cho, H. S., Choi, G., Choi, K. Y., and Oh, B. H. (1998) *Biochemistry* 37, 8325–8330.
5. Wu, Z. R., Ebrahimian, S., Zawrotny, M. E., Thornburg, L. D., Perez-Alvarado, G. C., Brothers, P., Pollack, R. M., and Summers, M. F. (1997) *Science* 276, 415–418.
6. Kim, S. W., Cha, S.-S., Cho, H.-S., Kim, J.-S., Ha, N.-C., Cho, M.-J., Joo, S., Kim, K.-K., Choi, K. Y., and Oh, B.-H. (1997) *Biochemistry* 36, 14030–14036.
7. Gerlt, J. A., and Gassman, P. G. (1993) *J. Am. Chem. Soc.* 115, 11552–11568.
8. Kuliopulos, A., Mildvan, A. S., Shortle, D., and Talalay, P. (1989) *Biochemistry* 28, 149–159.
9. Xue, L., Kuliopulos, A., Mildvan, A. S., and Talalay, P. (1991) *Biochemistry* 30, 4991–4997.
10. Zhao, Q., Abeygunawardana, C., Gittis, A. G., and Mildvan, A. S. (1997) *Biochemistry* 36, 14616–14626.
11. Thornburg, L. D., Henot, F., Bash, D. P., Hawkinson, D. C., Bartel, S. D., and Pollack, R. M. (1998) *Biochemistry* 37, 1049–10506.
12. Petrounia, I. P., and Pollack, R. M. (1998) *Biochemistry* 37, 700–705.
13. Massiah, M. A., Abeygunawardana, C., Gittis, A. G., and Mildvan, A. S. (1998) *Biochemistry* 37, 14701–14712.
14. Zhao, Q., Abeygunawardana, C., Talalay, P., and Mildvan, A. S. (1996) *Proc. Natl. Acad. Sci. U.S.A.* 93, 8220–8224.
15. Cleland, W. W., Frey, P. A., and Gerlt, J. A. (1998) *J. Biol. Chem.* 273, 25529–25532.
16. Kim, S. W., Kim, C. Y., Benisek, W. F., and Choi, K. Y. (1994) *J. Bacteriol.* 176, 6672–6676.
17. Bradford, M. M. (1976) *Anal. Biochem.* 72, 248–254.
18. Otwinowski, Z. (1993) in *Proceedings of the CCP4 Study Weekend* (Sawyer, L., et al., Eds.) pp 56–62, SERC Daresbury Laboratory, Warrington, U.K.
19. Luzzati, P. V. (1952) *Acta Crystallogr.* 5, 802–810.
20. Jones, T. A., and Kjeldgaard, M. (1991) *O*, version 5.9. The manual, Uppsala University, Uppsala, Sweden.
21. Kraulis, P. J. (1991) *J. Appl. Crystallogr.* 24, 946–950.
22. Lin, J., Westler, W. M., Cleland, W. W., Markley, J. L., and Frey, P. A. (1998) *Proc. Natl. Acad. Sci. U.S.A.* 95, 14664–14668.
23. Carter, P., and Wells, J. A. (1988) *Nature* 332, 564–568.
24. Cho, H. S., Ha, N. C., Choi, G., Kim, H. J., Lee, D., Oh, K. S., Kim, K. S., Lee, W., Choi, K. Y., and Oh, B. H. (1999) *J. Biol. Chem.* 274, 32863–32868.

BI991579K